Available online at www.sciencedirect.com
ScienceDirect
Scripta Materialia 58 (2008) 433–436
Scripta MATERIALIA
www.elsevier.com/locate/scriptamat

Friction stir lap joining aluminum and magnesium alloys

Y.C. Chen* and K. Nakata

Joining and Welding Research Institute, Osaka University, 11-1 Mihogaoka, Ibaraki, Osaka 567-0047, Japan

Received 26 September 2007; revised 16 October 2007; accepted 18 October 2007
Available online 26 November 2007

Al–Si and Mg–Al–Zn alloys were lap joined using friction stir welding during which the probe of a tool did not contact the surface of the lower Mg–Al–Zn alloy sheet. Micro X-ray diffraction was used to analyze phase transition in the joint. A conversion zone exists between the stir zone and the lower sheet metal which contained intermetallic compounds Al12Mg17, Al3Mg2 and Mg2Si. Using a lower welding speed resulted in no visible welding cracks and improved the joint strength.

Keywords: Friction stir welding; Aluminum alloy; Magnesium alloy; Micro X-ray diffraction

Aluminum alloys, which offer high strength, good formability and weight savings, are being considered for fabrication of vehicles. Magnesium alloys, the lightest of the structural metals, with a density two-thirds that of Al alloys, are a promising structural material in vehicle fabrication. In order to achieve a combination of the properties of Al and Mg alloys, development of reliable joints between Al alloys and Mg alloys is required. Thus, the problem of welding Al and Mg alloys must be faced. A variety of attempts to weld these alloys using fusion welding technology showed that this technique was not suitable because of the level of intermetallic compounds formed in the weld, which was deleterious to the mechanical properties [1,2].

As a solid-state welding technology, the friction stir welding (FSW) process [3] can weld Al alloys [4–11] and Mg alloys [12–16], and yields higher quality joints than those produced by fusion welding technology. These qualities are also expected when dissimilar metal materials are joined. Hirano et al. [17], Sato et al. [18] and Park et al. [19] investigated the friction stir weldability of Al alloy 1050 and Mg alloy AZ31. They reported the feasibility of a dissimilar high-quality weld of Al and Mg alloys. Microstructural analysis results showed that the intermetallic compound Al12Mg17 was formed in the weldment. Somasekharan and Murr [20] reported the friction stir weldability of Mg alloy AZ31B/AZ91D and Al alloy 6061-T6. The weld zone showed unique dissimilar weld, but the microhardness distribution in the weld was uneven and erratic hardness spikes exhibited hardness values as much as three times that of the base material hardness. Mclean et al. [21] reported the results of FSW of Mg alloy AZ31B to Al alloy 5083. They showed that visually sound welds could be produced. However, the formation of a thin intermetallic layer at the interface resulted in welds that exhibited virtually no ductility. The intermetallic layer was identified as Al12Mg17.

The current literature on FSW of Al and Mg alloys mainly concerns research into friction stir butt joints; friction stir lap joining of Al alloys and Mg alloys has not been reported. From the industrial application point of view, development of reliable investigation is meaningful. In this study, AC4C cast Al and AZ31 Mg alloys have been selected as the experimental materials for friction stir lap welding. The insert depth of a tool is strictly controlled to less than the thickness of the upper sheet. The emphasis is placed on the tensile strength, fracture location of the joint and the microstructure evolution in the weld under different welding heat inputs.

The base material used in this study was a 3 mm thick AC4C cast Al alloy sheet with composition of Al–0.3Mn–0.15Fe–0.2Ca–7.5Si (wt.%) and a 2.5 mm thick AZ31 Mg alloy sheet with a composition of Mg–3Al–1Zn–0.2Mn (wt.%). The sheet was cut and machined into rectangular welding samples, 300 mm long by 100 mm wide, which were longitudinally lap-welded using a FSW machine. The Al alloy sheet was put on the Mg alloy sheet. The relative position of Al alloy and Mg alloy in transverse direction is shown in Figure 1.

* Corresponding author. Tel./fax: +81 6 6879 8668; e-mail: armstrong@hit.edu.cn

1359-6462/$ - see front matter
doi:10.1016/j.scriptamat.2007.10.033

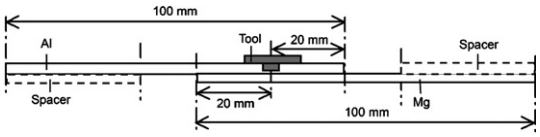

Figure 1. A schematic plan of the relative position of Al alloy, Mg alloy and the tool.

The welding parameters were: rotation speed 1500 rpm; welding speeds 20, 50 and 80 mm min^{-1}. The upsetting force of the welding tool (SKD61 tool steel) used in this experiment was 5.88 kN. The shoulder diameter and probe diameter of the tool were 15 and 5 mm, respectively. The length of the probe was 2.6 mm and the welding tilt angle was 3°.

After welding, the joint was cross-sectioned perpendicular to the welding direction for the metallographic analyses and tensile tests using an electrical-discharge cutting machine. The cross-sections of the metallographic specimens were polished with diamond polishing agent, etched in a 5 ml acetic acid + 6 g picric acid + 10 ml water + 100 ml ethanol solution and observed by optical microscopy.

The mechanical properties of the joint were measured using tensile tests. The tensile tests were carried out at room temperature at a crosshead speed of 1 mm min^{-1} using a tensile testing machine, and the mechanical properties of the joint were evaluated using three tensile specimens cutting from the same joint. The shape of the test specimen was rectangular and the width of each specimen was 20 mm.

The interface structure and element distribution in the weld were analyzed by scanning electron microscopy (SEM) equipped with an energy-dispersive X-ray spectroscopy (EDS) analysis system. The localized phase structure in the weld was determined using micro X-ray diffraction (micro-XRD). Micro-XRD (D8 Discover, Bruker-axs Ltd., Japan) was performed with Cu K_α radiation at 45 kV and a relatively high tube current of 110 mA. The diameter of the analysis area used in this study was 0.1926 mm. The analysis angles ranged from 20° to 110°.

Figure 2 shows the cross-sections of joints at different welding speeds. The relative position of the tool during welding is shown in the joint. From Figure 2 we can see that although the length of the probe is shorter than the thickness of the upper Al sheet, Al in the stir zone has been deeply embedded into the lower Mg sheet because of the softening of the lower Mg sheet. Moreover, a heavy conversion zone is formed at the interface.

The lower the welding speed, the thicker the conversion zone. For FSW, lower welding speed means more heat input, which provides better conditions for reaction diffusion of Al and Mg and results in a thicker conversion zone. Meanwhile, the microstructure in the stir zone is significantly different under different welding conditions. The stir zone contains a large, irregularly shaped region when the welding speed is 20 mm min^{-1} (see Fig. 2b). The irregularly shaped structure is distributed from the interface to the surface of the joint. However, this irregularly shaped region is not observed when the welding speed is 80 mm min^{-1} (see Fig. 2a). The

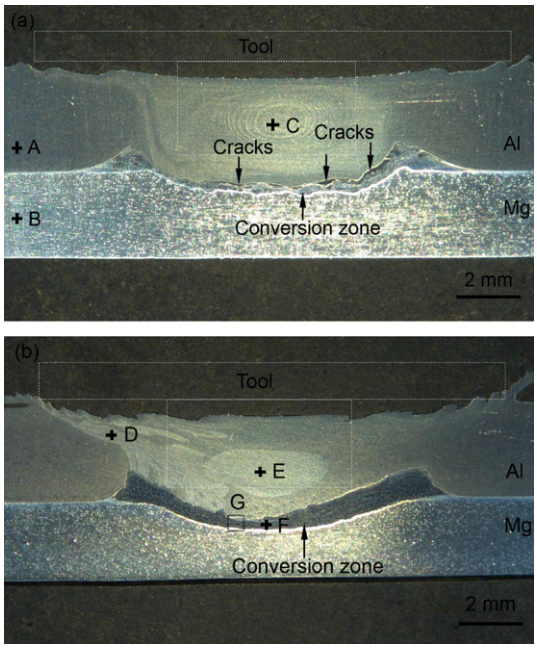

Figure 2. Cross-section of joints: (a) 80 mm min^{-1}, (b) 20 mm min^{-1}.

phase structure in this irregularly shaped region was determined using micro-XRD and the results are shown below. In addition, cracks are found at the interface between the stir zone and the conversion zone when the welding speed is 80 mm min^{-1} (see Fig. 2a), but no visible welding cracks appear in the joint when the welding speed is 20 mm min^{-1} (see Fig. 2b). Such cracks have a significant effect on the tensile properties of joints.

The tensile test results of joints are shown in Figure 3. The failure loads of all joints are lower than those of base materials and all the joints fracture at the interface.

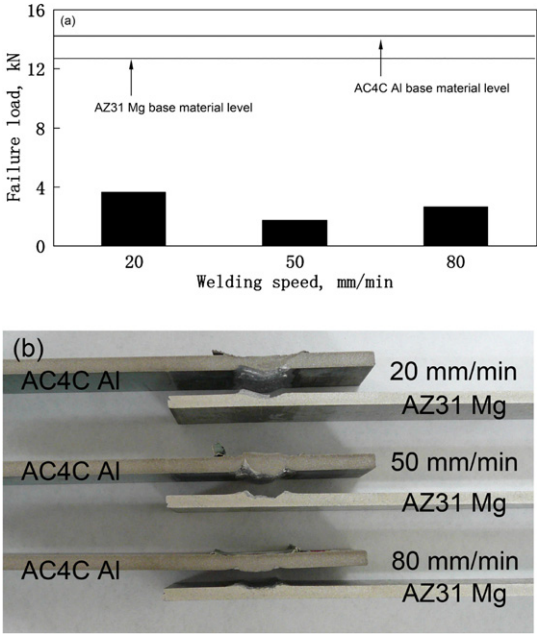

Figure 3. Failure loads and fracture locations of joints: (a) failure load, (b) fracture location.

The joints exhibit no ductility. The maximum failure load, 3.63 kN, is obtained at a welding speed of 20 mm min^{-1}. Failure loads of joints show lower values when higher welding speeds are carried out. This is probably due to welding cracks in the joint, which provide a source of cracking during tensile testing.

Micro-XRD spectra obtained from different locations (Fig. 2) are indicated in Figure 4. Figure 4a shows the micro-XRD spectra obtained from locations A, B and C. The micro-XRD result from location A shows that AC4C Al alloy mainly contains Al and Si phases because AC4C Al alloy is a hypoeutectic Al–Si alloy. The micro-XRD pattern from location B indicates the presence of the Mg phase in AZ31 Mg alloy base material. The result from location C, the stir zone center, shows that the phases in this region are Al and Si. That is, the phase structures in the stir zone do not change after welding.

Figure 4b shows the micro-XRD spectra obtained from locations D, E and F. The micro-XRD results from locations D and E show that the irregularly shaped region mainly contains Al, Si and Mg2Si phases. The presence of the Mg2Si phase in the weld indicates that a certain amount of stir behavior occurs at the interface and entraps some Mg into the stir zone when a lower welding speed is used, resulting in the formation of a large number of Mg2Si phases. The micro-XRD pattern from location F shows that large peaks of intermetallic compounds Al12Mg17, Al3Mg2 and Mg2Si are detected, though this pattern contains some peaks

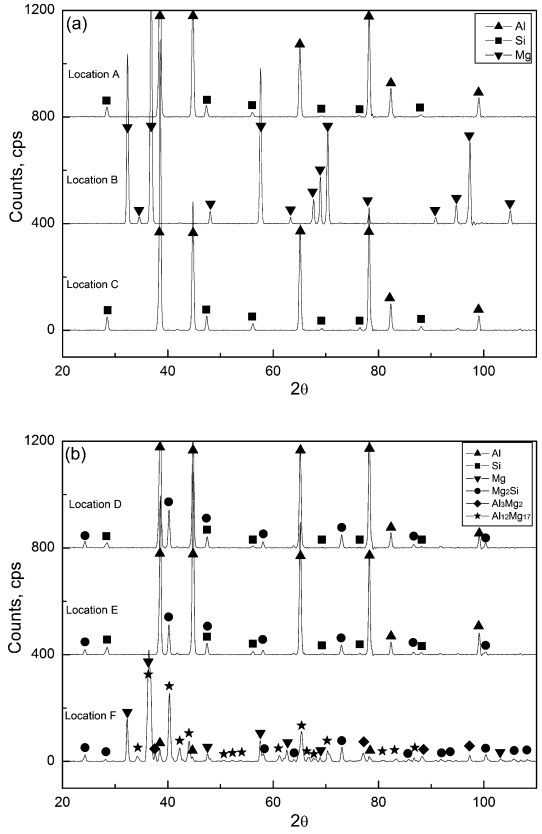

Figure 4. Micro-XRD spectrums from different locations shown in Figure 2: (a) locations A, B and C; (b) locations D, E and F.

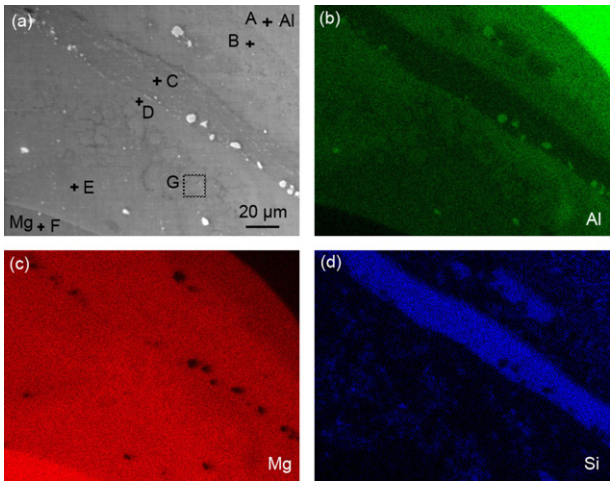

Figure 5. Qualitative EDS analysis of the interface layer: (a) SEM image, (b) Al, (c) Mg, (d) Si.

obtained from matrices. The micro-XRD results confirm that reaction diffusion takes place at the interface between the AC4C Al stir zone and the lower AZ31 Mg sheet.

A SEM micrograph of the interface (region G in Fig. 2b) is shown in Figure 5a. Al, Mg and Si distributions are shown in Figure 5b–d. These results show that the conversion zone contains lamellar structures involving Al, Mg and Si. Quantitative chemical compositions analysis results from position A to position F by EDS are shown in Table 1.

Point A (stir zone on the Al side) contains 4.18 wt.% Mg, suggesting that Mg element is involved in the Al stir zone. The intervention of Mg element leads to the formation of an irregularly shaped region in the weld (see Fig. 2b). Point B is composed of 60.39 wt.% Al, 35.51 wt.% Mg and 4.10 wt.% Si, indicating that this location may contain Al3Mg2 and Mg2Si intermetallic compounds.

Point C lies in a Si-rich band. EDS shows that it contains as much as 20.31 wt.% Si. This value is much higher than that in AC4C base material (7.5 wt.% Si), indicating that plenty of Si element clusters in this region because of a certain amounts of stirring during welding. This finding, combined with the XRD analysis results shown in Figure 4b, indicates that this region should mainly contain the intermetallic compound Mg2Si.

Quantitative analysis of the chemical compositions of points D and E shows that these two positions mainly contain Al and Mg element. From the ratio of Al to Mg it can be seen that these two regions mainly contain

Table 1. Elemental analysis results of the interface layer

Position	Element (wt.%)		
	Mg	Al	Si
A	4.18	91.25	4.57
B	35.51	60.39	4.10
C	51.83	27.86	20.31
D	54.95	43.07	1.99
E	67.16	32.11	0.73
F	89.09	10.64	0.27

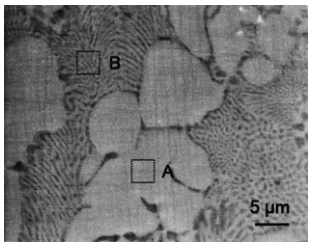

Figure 6. SEM image and qualitative EDS analysis of the eutectic region.

the intermetallic compound Al12Mg17 and Mg solid solution. Point F lies on the Mg side and contains 89.09 wt.% Mg and 10.64 wt.% Al, suggesting that some Al element diffuses into the Mg matrix.

A magnified SEM image of part of the interface (region G in Fig. 5a) is shown in Figure 6. It appears that this region has a solidified microstructure. Two kinds of phases are included in this region: a white massive phase (position A) and a black and white lamellar phase (position B). Quantitative analysis of the chemical compositions by EDS shows that the white phase consists of 58.55 wt.% Mg and 41.45 wt.% Al, while the black and white phase contains 65.55 wt.% Mg and 34.45 wt.% Al. This result suggests that the white phase is the intermetallic compound Al12Mg17 and the black and white phase is a eutectic mixture of Al12Mg17 and Mg solid solution.

Friction stir lap joining of AC4C Al alloy and AZ31 Mg alloy produces a conversion zone at the interface, which results in the joining of Al alloy AC4C and Mg alloy AZ31 when the probe of a tool does not contact the surface of lower Mg sheet. Results from micro-XRD, SEM and EDS suggest that the conversion zone has a solidified microstructure experiencing the eutectic reaction: liquid $\rightarrow$ Al12Mg17 + Mg, after the primary solidification of Al12Mg17. As Sato et al. [18] suggested in a previous study on friction stir butt joining of 1050 Al alloy and AZ31 Mg alloy, it is possible that constitutional liquefaction occurs during friction stir welding. The present lap joint should be exposed to peak temperatures higher than 723 K (the liquid-phase formation temperature) during the stirring, because temperature measurement by thermocouples shows that the peak temperature exceeds 723 K during FSW of AC4C Al alloy at the same welding parameters. The peak temperature is sufficient for mutual diffusion between Al and Mg atoms and for the formation of a liquid phase. The eutectic reaction occurs during the solidification of the liquid phase, which then forms Al12Mg17 and Mg solid solution after the primary solidification of Al12Mg17. According to the Al–Mg binary phase diagram [22], Al3Mg2 phase can be produced through peritectoid reaction of Al and Al12Mg17. Because the conversion zone is mainly composed of brittle phases of Al3Mg2 and Al12Mg17, the joints exhibit no ductility during tensile testing. Moreover, welding cracks occur at the interface when a higher welding speed is used. As mentioned above, constitutional liquefaction occurred at the interface during FSW. Thus, cooling speed undoubtedly affects the formation of welding cracks. A higher cooling speed (i.e. higher welding speed) causes higher stress concentration at the interface and results in welding cracks during cooling. From the point of view of restraining crack formation, lower welding speeds should be used.

In summary, the following conclusions are reached. Firstly, AC4C Al alloy and AZ31 Mg alloy can be lap welded using FSW technology when the tip of probe does not touch the surface of the bottom Mg sheet. The two sheets are joined through conversion zone at the joint interface. Secondly, constitutional liquefaction occurs in the joint during welding and the intermetallic compounds Al12Mg17, Al3Mg2 and Mg2Si are produced at the interface. Finally, using a lower welding speed results in no visible welding cracks in the joint and improves the joint strength.

[1] A. Ben-Artzy, A. Munitz, G. Kohn, B. Brining, A. Shtechman, Magnesium Technol. (2002) 295–302.
[2] L. Liu, H. Wang, G. Sone, J. Ye, J. Mater. Sci. 42 (2007) 565–572.
[3] W.M. Thomas, E.D. Nicholas, J.C. Needham, M.G. Murch, P. Templesmith, C.J. Dawes, GB Patent Application No. 9125978.8, December 1991.
[4] C.G. Rhodes, M.W. Mahoney, W.M. Bingel, R.A. Spurling, W.H. Bampton, Scripta Mater. 36 (1997) 69–75.
[5] M.W. Mahoney, C.G. Rhodes, J.G. Flintoff, R.A. Spurling, W.H. Bampton, Metall. Mater. Trans. A 29A (1998) 1955–1964.
[6] Y.S. Sato, H. Kokawa, M. Enomoto, S. Jogan, Metall. Mater. Trans. A 30A (1999) 2429–2437.
[7] Y.S. Sato, H. Kokawa, M. Enomoto, S. Jogan, T. Hashimoto, Metall. Mater. Trans. A 30A (1999) 3125–3130.
[8] K.V. Jata, S.L. Semiatin, Scripta Mater. 43 (2000) 743–749.
[9] Y.S. Sato, S.H.C. Park, H. Kokawa, Metall. Mater. Trans. A 32A (2001) 3033–3042.
[10] Y.S. Sato, H. Kokawa, Metall. Mater. Trans. A 32A (2001) 3023–3031.
[11] G.M.D. Cantin, S.A. David, W.M. Thomas, E. Lara-Curzio, S.S. Babu, Sci. Technol. Weld. Join. 10 (2005) 268–280.
[12] S.H.C. Park, Y.S. Sato, H. Kokawa, Scripta Mater. 49 (2003) 161–166.
[13] D. Zhang, M. Suzuki, K. Maruyama, Scripta Mater. 52 (2005) 899–903.
[14] A.H. Feng, Z.Y. Ma, Scripta Mater. 56 (2007) 397–400.
[15] C.I. Chang, C.J. Lee, J.C. Huang, Scripta Mater. 51 (2004) 509–514.
[16] W. Woo, H. Choo, D.W. Brown, P.K. Liaw, Z. Feng, Scripta Mater. 54 (2006) 1859–1864.
[17] S. Hirano, K. Okamoto, M. Doi, H. Okamura, M. Inagaki, Y. Aono, Quart. J. Jpn. Weld. Soc. 21 (2003) 539–545.
[18] Y.S. Sato, S.H.C. Park, M. Michiuchi, H. Kokawa, Scripta Mater. 50 (2004) 1233–1236.
[19] S.H.C. Park, M. Michiuchi, Y.S. Sato, H. Kokawa, in: Proceedings of the International Welding/Joining Conference, Korea 2002, KWS, Gyeongju, 2002, pp. 534–538.
[20] A.C. Somasekharan, L.E. Murr, Mater. Charact. 52 (2004) 49–64.
[21] A.A. McLean, G.L.F. Powell, I.H. Brown, V.M. Linton, Sci. Technol. Weld. Join. 8 (2003) 462–464.
[22] J.L. Murray, in: Phase Diagrams of Binary Magnesium Alloys, ASM International Materials Park, OH, 1988, p. 17.